Chapter 5

Heterojunction Barrier Varactor Diodes

In this chapter we will examine an alternative approach for generating submillimeter-wavelength radiation: frequency multiplication with a varactor diode. The dominant semiconductor device presently used for such applications is the Schottky barrier diode. However, due to certain limitations that will be discussed, there is interest in developing alternate heterostructure based varactors. One such device is the Heterojunction Barrier Varactor (HBV) diode. The major problem with this type of device is its low breakdown voltage and excessive conduction current which leads to low multiplier conversion efficiency. We address in this chapter the issue of increasing the breakdown voltage by examining HBV diodes fabricated in the AlAs/$In_{0.53}Ga_{0.47}As$ and low growth temperature AlGaAs material systems.

5.1 Introduction to varactor frequency multiplication

As we have seen in the previous chapter, DBRTD oscillators will not be able to deliver the required output power (1 mW) at submillimeter-wavelengths. Therefore, frequency multiplication of a high power, lower frequency source must be employed. Frequency multiplication or harmonic generation is a nonlinear process and is widely used in such electronic instrumentation as digital sampling oscilloscopes and spectrum analyzers. This technique involves " pumping" a nonlinear element with a RF source at a pump frequency, f_p, with the nonlinear element converting this power at the pump frequency to some higher nth order harmonic frequency, f_n. There are two methods of harmonic generation: resistive and reactive multiplication.

A resistive multiplier, or a varistor, achieves harmonic generation through a nonlinear resistance such as with a p-n junction diode in the " knee" region in

forward bias. However, frequency multiplication with a varistor is very inefficient due to resistive power losses. Page has shown than a varistor's maximum power conversion efficiency from f_p to f_n is given by [1]

$$P_n = \frac{1}{n^2} P_1 \tag{5.1}$$

where P_1 is the input power and P_n is the output power at the desired nth harmonic. Therefore, the maximum power conversion efficiency with a resistive tripler, for example, is 11%. A more efficient method is use to a varactor or a reactive multiplier where the efficiency can (theoretically) approach 100% [2]. The nonlinear reactance is typically capacitive and frequency multiplication with an ideal, lossless capacitor can be understood by representing the displacement current through the capacitor, $i_d(t)$, as

$$i_d(t) = \frac{d}{dt}\big(C(V) * V(t)\big) = \frac{dV}{dt}\left(C(V) + V\frac{dC}{dV}\right) \tag{5.2}$$

where

$$C(V) = C_0 + \big(V - V_0\big)\frac{dC}{dV}\bigg|_{V=V_0} + \frac{\big(V - V_0\big)^2}{2}\frac{d^2C}{dV^2}\bigg|_{V=V_0} + ... \tag{5.3}$$

Therefore, the strength of the harmonic components of the capacitor displacement current are dependent on three factors. The first factor is, of course, the capacitance nonlinearity through the dC/dV terms in Eqs. 5.2 and 5.3. The harmonic strength also depends on the magnitude of the DC bias voltage and RF pump voltage through V_0 and V(t), respectively. The third factor determining the strength of the harmonics is the frequency of the pump voltage through the dV/dt term.

The above treatment is a small-signal analysis that gives an intuitive feel for the factors important in varactor frequency multiplier. In practice, however, calculation of the conversion efficiency requires a large signal analysis taking into account the embedding circuit into which the varactor diode is placed.

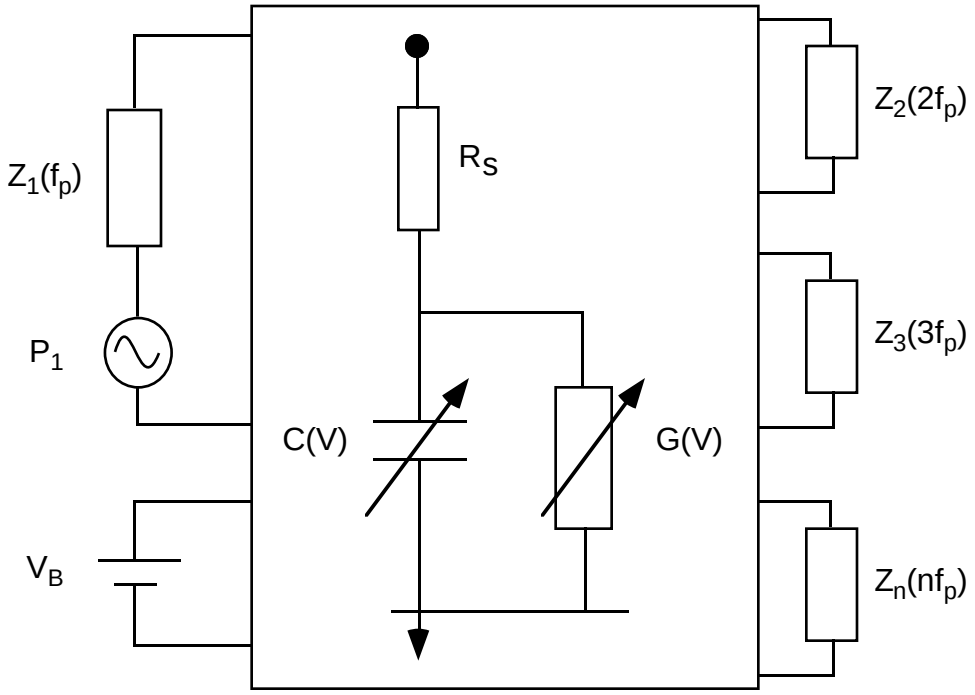

Fig. 5.1 Equivalent circuit of a varactor frequency multiplier including the embedding impedances, $Z_n(nf_p)$, which function as idler circuits. The varactor diode equivalent circuit is shown in the inset and is given by a parallel combination of a voltage dependent capacitance, C(V), and conductance, G(V), in series with a parasitic series resistance, R_s. V_B is the bias voltage and Z_1 is the input impedance. This figure is adapted from Tolmunnen *et al.*, Int. Journal of Infrared and Millimeter Waves, vol. 12, No. 10, pp.1111-1133, 1991.

An equivalent circuit [3] of the multiplier embedding circuit and the varactor diode is given in Fig. 5.1. The varactor diode equivalent circuit is shown in the inset and is given by a parallel combination of a voltage dependent

capacitance, C(V), and conductance, G(V), in series with a parasitic series resistance, R_s. The conductance G in the circuit accounts for the leakage current in a non-ideal capacitor. The parasitic series resistance includes contributions from ohmic contacts, undepleted epi-layer, and spreading resistance. The embedding impedances, Z_n, called idler circuits, are designed to provide a reactive load at all harmonics but the desired one so that power is only delivered at the desired harmonic. Designing such lossless idler circuits is very difficult, especially at millimeter and submillimeter wavelengths, and in general, power losses in the idler circuitry limit the order of frequency multiplication of a varactor multiplier [4]. Accurate computation of the multiplier conversion efficiency requires using harmonic balance analysis, which involves dividing the multiplier circuit into linear and nonlinear sub circuits, which are then analyzed in the frequency and time domains, respectively [5].

Since the primary concern of this work is the varactor diode characteristics, the following discussion will focus on device design aspects only. However, it must kept in mind that the overall success of a particular device design depends on how well it performs in an actual multiplier circuit.

For efficient varactor operation the reactance of the varactor capacitance must be much larger than the device series resistance. If we assume ideal capacitor characterisitcs (G = 0) but with a parasitic series resistance, R_s, then one can determine a figure of merit, the dynamic cutoff frequency, f_c [6] as

$$f_c = \frac{1}{2\pi R_s}\left(\frac{1}{C_{\min}} - \frac{1}{C_{\max}}\right) \tag{5.4}$$

where C_{min} and C_{max} are the minimum and maximum values of the device capacitance, respectively, during the RF cycle. From Eq. 5.4 we see that for achieving a high f_c, the device area should be very small (minimize C_{min} and C_{max})

and have very low series resistance. Another figure of merit is given by a characteristic frequency ω_g

$$\omega_g = \frac{G}{C} \tag{5.5}$$

where G and C are the device's shunt conductance and capacitance, respectively. Such a parameter gives a measure of the diode's current blocking capability since it is a ratio of the conduction current to the displacement current. Therefore, for $\omega > \omega_g$, the device behaves more like a capacitor, whereas, for $\omega < \omega_g$, it behaves more like a varistor. For efficient varactor operation, one would prefer ω_g to be as small as possible.

5.2 Schottky Diode Varactors

There are several devices that will function as varactor frequency multipliers since all that is really required is that the device exhibit a nonlinear capacitance. For example, p-n junction diodes and MOS capacitors can be employed. However, these devices have limited application at millimeter wavelengths due to minority carrier charge storage effects [7]. More recently there has been some development in heterostructure-based varactors such as the BIN diode [8] and the Schottky/HEMT diode varactors [9]. These devices suffer from low breakdown voltages and cutoff-frequencies and are not being pursued for submillimeter wavelength applications [10]. For submillimeter wave frequency multiplication, the GaAs Schottky barrier diode is the dominant technology . This is due to the low shunt conductances and high breakdown voltages that can be achieved.

A Schottky barrier varactor diode consists of a circular metallic contact deposited on a lightly doped, epitaxially grown n-type layer. The GaAs substrate is heavily doped to minimize parasitic series resistance. The top contact surface area of submillimeter wavelength Schottky diodes is typically about 0.1 μm^2 with a

zero-bias junction capacitance of 0.25 fF [11]. The diode is placed on a waveguide post with a sharply pointed whisker contacting the top anode.

Erickson reported obtaining 700 μW at 474 GHz with 3% conversion efficiency [12]. This source consisted of a cascaded Schottky diode doubler and tripler and was pumped by an InP Gunn diode oscillator producing 120 mW at 79 GHz. More recently, Rydberg *et al.* reported a 800 GHz Schottky diode varactor frequency tripler that produced 120 μW with a tripler conversion efficiency of 0.8% [13]. Although these output powers and conversion efficiencies are very impressive, they still fall short of the one to five milliwatt LO power requirement of the terahertz Schottky diode mixer.

One of the factors contributing to the difficulty in obtaining sufficient power and conversion efficiency is the substantial resistive loss in the idler circuitry. Since the capacitance-voltage characteristics of the Schottky diode are asymmetric with respect to voltage, all higher order harmonics are generated. Therefore, if a quintupler (x 5 multiplier) is to be designed, lossless idler circuitry are required at the second, third, and fourth harmonics to prevent power from being dissipated at these undesired harmonics. Designing such circuitry, as mentioned earlier, is an especially daunting task at submillimeter wavelengths. Therefore, it is desirable to be able to reduce the number of idler circuits and consequently achieve higher conversion efficiencies and output powers.

5.3 HBV Frequency Multipliers

Kollberg *et al.* at Chalmers University recently reported a new type of varactor, the heterojunction barrier varactor (HBV) diode whose layer schematic, equilibrium conduction energy band, and C- V characteristic is shown in Fig. 5.2 [14]. The device is essentially a single barrier structure sandwiched between long, moderately doped depletion regions. When the diode is biased in one direction, one of the drift regions will become depleted and the depletion capacitance of the

device will decrease with increasing voltage. Since the diode is a symmetric structure, a reverse bias will also result in a decrease in capacitance. Consequently, the C- V characteristic will exhibit a peak at zero applied voltage and decrease with increasing bias as shown in Fig. 5.2. The heterojunction barrier prevents conduction current from passing through the device and degrading the multiplier conversion efficiency. Therefore, this device is similar to the Schottky barrier varactor diode in that both consist of a current blocking barrier and a depletion region whose width is a function of the applied voltage. However, since the HBV C - V characteristic is symmetric with respect to voltage, Eq. 5.3 becomes

$$C(V) = C_0 + \frac{(V - V_0)^2}{2} \left. \frac{d^2 C}{dV^2} \right|_{V=0} + even\,terms \qquad (5.6)$$

If V(t) = sinωt, we can see that substituting Eq. 5.6 into Eq. 5.2 results in the current through the capacitor having only odd harmonics. Therefore, the additional symmetry in the C - V characteristics reduces the number of generated harmonics by a factor of two. Going back to the quintupler example, an HBV diode would only require an idler at the third harmonic, thereby reducing expensive and difficult circuit design and eliminating losses due to unoptimized idler terminations. Furthermore, the HBV has an advantage over Schottky barrier varactors due to their ability to be "bandgap" engineered for improved nonlinear C - V and I - V characteristics.

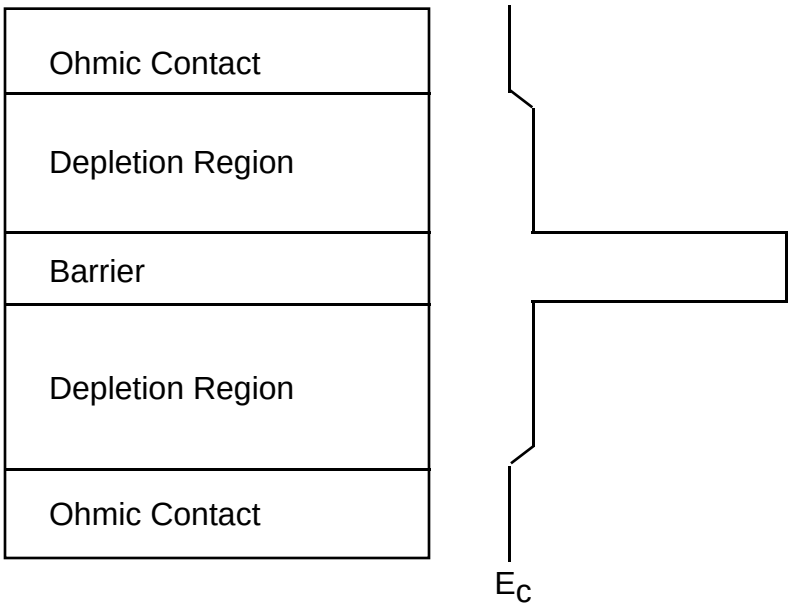

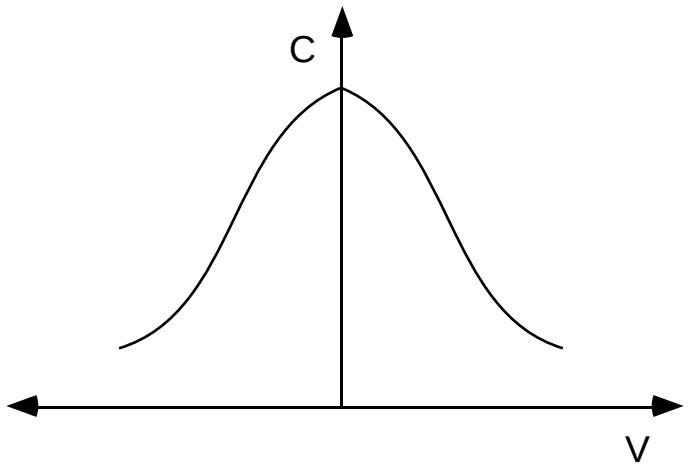

Fig. 5.2 Layer schematic, equilibrium conduction energy band diagram, and C - V characteristic of heterojunction barrier varactor (HBV) diode.

It should be pointed out that the DBRTD can also be used as a symmetric frequency multiplier [15] since it its I - V curve is also symmetric about the origin. Furthermore, because of its NDR the DBRTD multiplier's theoretical efficiency is greater than the $1/n^2$ value that applies to normal diodes. However, DBRTD multipliers have not been successful at millimeter wavelengths and lower and it has been determined that the harmonic generation in these devices is due primarily to the voltage variable capacitance rather than the resistance [16], [17]. Schottky diode varactors can also generate symmetric C - V characteristics if they are connected in series (back-to-back). Frequency doublers employing back-to-back Schottky diodes in a planar array have been reported to achieve 55 mW at 175 GHz [18]. However, such an approach is not feasible at submillimeter wavelengths due to the large parasitic pad capacitance inherent in such structures.

The symmetric C - V characteristic of the HBV diode has generated a great deal of interest in the submillimeter wavelength research community and several groups have reported HBV multiplier results at millimeter and submillimeter wavelengths. Rydberg *et al.* obtained 2 mW and 5% conversion efficiency with a tripler to 280 GHz [19]. These tripler results are approximately the same as can be achieved using state-of-the-art Schottky varactor diodes in the same tripler mount. Choudhury *et al.* also reported tripler results at 200 GHz with an output power of 0.8 mW and 5% conversion efficiency [20]. The HBV diodes used in both experiments were nominally identical and were grown at Chalmers University. These single barrier devices consisted of a nominally undoped 210Å $Al_{0.7}Ga_{0.3}As$ single barrier sandwiched between 5300Å GaAs depletion layers having a doping concentration of 1×10^{17} cm^{-3}. The top and bottom contact layers are formed with heavily doped ($n = 3.4 \times 10^{18}$ cm^{-3}) GaAs layers. Liu *et al.* have recently reported a monolithic quasi-optical frequency tripler array [21] consisting of 3000 diodes. They obtained 5 W at 99 GHz with a conversion efficiency of 2%. The devices were connected in a back-to-back fashion and the device layer sequence consisted of three $Al_{0.7}Ga_{0.3}As$ single barriers separated by 1500Å ($n = 1 \times 10^{17}$ cm^{-3}) depletion regions with a top-side Schottky contact. Since the devices are in series,

the number of barriers is doubled to six. Such a stacked barrier approach reduces the power dropped across each barrier, thus improving the power handling capability of each device [22].

However, the multiplier performance of the above devices is limited by excessive conduction current [23]. This large parasitic conductance reduces the multiplier efficiency since the devices are acting more like varistors rather than varactors. Furthermore, the devices have breakdown voltages as low as two to three volts which limits their power handling capability. Therefore, if HBV multiplier performance is to be improved, the current blocking characteristics must be improved which will consequently improve the HBV power handling capability and relax circuit design requirements.

From the discussion of section 3.4, it comes as no surprise that the device performance of the single barrier $Al_{0.7}Ga_{0.3}As$ HBV diode is limited by excessive conduction current. It is well established that for indirect bandgap barriers, X-point mediated transport is very important, especially in thick (greater than 30Å), Al-rich ($x > 0.45$) barriers [24], [25]. Therefore, alternative device designs and material systems must be investigated to improve the breakdown characteristics and reduce the excess conduction current.

5.4 AlGaAs/GaAs HBV Diodes

One technique to reduce X-point mediated current is to use the " chair" barrier concept discussed in Chapter 3. Shown in Fig. 5.3 is the layer schematic of an $Al_{0.35}Ga_{0.65}As$/AlAs/GaAs " chair" barrier structure along with the conduction band energy diagram. The " chair" barrier consists of a 50Å $Al_{0.35}Ga_{0.65}As$ layer sandwiching a 100Å AlAs layer. The barrier is surrounded on both sides with 4000Å ($n = 1.1 \times 10^{17}$ cm^{-3}) GaAs depletion layers. The depletion region length and doping concentration chosen are similar to what are used in submillimeter wavelength Schottky diode varactors [26].

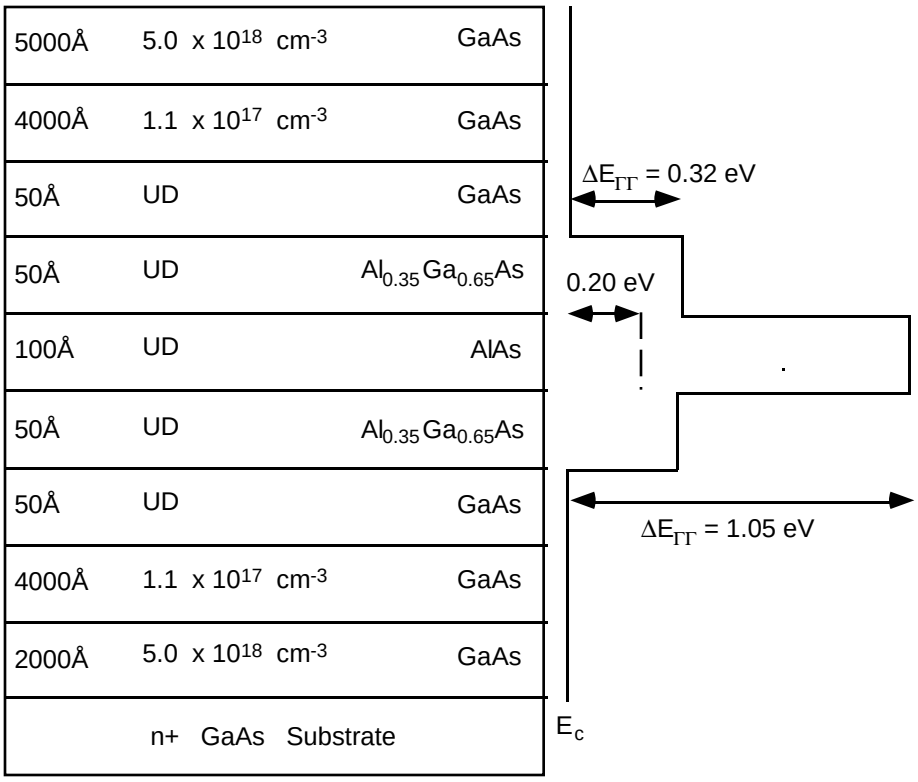

Fig. 5.3 Layer schematic of a $Al_{0.35}Ga_{0.65}As$/AlAs/GaAs " chair" barrier HBV diode along with conduction band energy diagram. The barrier heights are from Adachi [27].

The $Al_{0.35}Ga_{0.65}As$ Γ - Γ barrier height of 0.32 eV is larger than the 0.2 eV Γ - X barrier height between AlAs and GaAs. Therefore, the Γ - X mediated current through the thick (100Å) AlAs layer should be reduced due to the "screening" effect of the direct bandgap $Al_{0.35}Ga_{0.65}As$ layer.

Another approach to improve current blocking is to use low growth temperature GaAs (LT-GaAs). It has been shown by Smith *et al.* that the MBE growth of GaAs at substrate temperatures in the range of 150 to 350°C, followed by an anneal at 600°C in an arsenic ambient, results in layers exhibiting very high resistivity [28]. Arsenic precipitates form in the LT-GaAs layer and contribute to

the semi-insulating behavior. For a thorough review regarding this interesting material the reader is referred to [29]. Rogers *et al.* recently employed a LT-$Al_{0.67}Ga_{0.33}As$ layer as a current blocking layer in a vertical cavity laser structure [30]. The use of LT-AlGaAs layers is preferred to LT-GaAs since higher resistivity can be obtained [31]. Shown in Fig. 5.4 is the layer schematic of three LT-$Al_{0.52}Ga_{0.48}As$ HBV diodes with L, the LT-$Al_{0.52}Ga_{0.48}As$ barrier thickness, equal to 250Å, 500Å, and 750Å. The LT-$Al_{0.52}Ga_{0.48}As$ barrier is sandwiched between 3000Å ($n = 8.8 \times 10^{16}$ cm^{-3}) GaAs depletion regions. The J - V characteristics of the LT-$Al_{0.52}Ga_{0.48}As$ and the "chair" barrier HBV diodes are given in Fig. 5.5. The "chair" barrier HBV has the lowest breakdown voltage, approximately 3 V. The LT-$Al_{0.52}Ga_{0.48}As$ HBV diodes have breakdown voltages of about 6 V, 10V, and 12V for L = 250Å, 500Å, and 750Å, respectively. The slight asymmetry in the J - V characteristics of the LT-$Al_{0.52}Ga_{0.48}As$ devices is probably due to the MBE growth process since growth is interrupted to change the substrate temperature from 600°C to 250°C. Nevertheless, it is clear that increasing the LT-$Al_{0.52}Ga_{0.48}As$ layer thickness improves current blocking. However, as the barrier thickness increases the capacitance modulation ratio will decrease. So, it is necessary that the capacitance modulation ratio not be sacrificed in the quest for improved current blocking. Therefore, the same level of current blocking must be achieved with thinner barriers. This is possible if one employs the $AlAs/In_{0.53}Ga_{0.47}As$ material system as will be shown in the next section.

5000Å	4 x 10^{18} cm^{-3}	GaAs
3000Å	8.8 x 10^{16} cm^{-3}	GaAs
50Å	UD	GaAs
L	UD	$Al_{0.52}Ga_{0.48}As$
50Å	UD	GaAs
3000Å	8.8 x 10^{16} cm^{-3}	GaAs
2500Å	4 x 10^{18} cm^{-3}	GaAs
n+ GaAs Substrate		

Fig. 5.4 Layer schematic of LT-$Al_{0.52}Ga_{0.48}As$ HBV Diode. L = 250Å, 500Å, and 750Å.

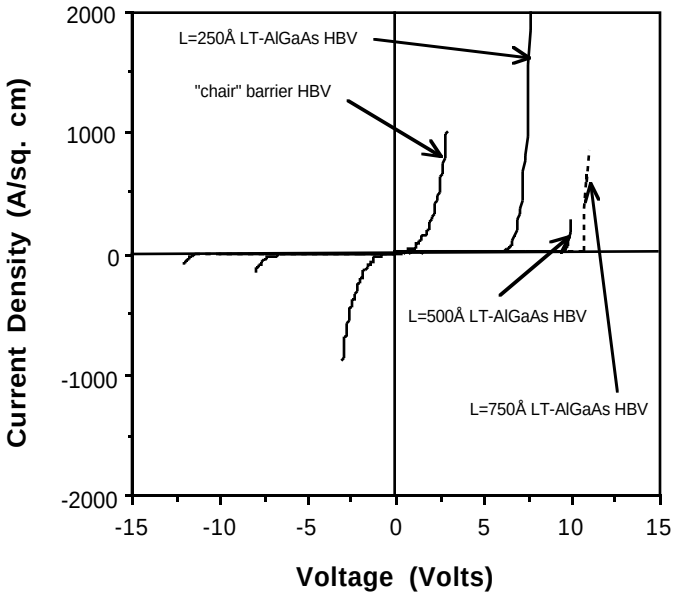

Fig. 5.5 J - V characteristics of LT-$Al_{0.52}Ga_{0.48}As$/GaAs and "chair" barrier $Al_{0.35}Ga_{0.65}As$/AlAs/GaAs HBV diodes.

5.5 AlAs/$In_{0.53}Ga_{0.47}As$ HBV Diodes

Since the Γ-X mediated current is the dominant parasitic current transport in the AlGaAs/GaAs HBV diodes discussed in the previous sections, one obvious solution is to fabricate HBV diodes in the AlAs/$In_{0.53}Ga_{0.47}As$ material system since it offers a much higher Γ-X barrier height. The current transport mechanism contributing to the conduction current in the single barrier devices is similar to that contributing to the valley current in DBRTDs. Therefore, the success of the AlAs/$In_{0.53}Ga_{0.47}As$ material system in increasing the PVCR of DBRTDs should also be applicable to improving the current blocking in HBV diodes.

Three AlAs/$In_{0.53}Ga_{0.47}As$ HBV diodes were fabricated and characterized. The layer schematic of the three HBV structures is shown in Fig. 5.6, where L denotes the thickness of the barrier and BARRIER represents its composition. For the first device, HBV I, L = 50Å and BARRIER = AlAs. The second device, HBV II, has L = 100Å and BARRIER = AlAs. For the third structure, HBV III, L = 50Å/50Å/50Å and BARRIER = $In_{0.52}Al_{0.48}As$/AlAs/$In_{0.52}Al_{0.48}As$. The capacitance modulation is obtained through the depletion of the 3000Å (1.2×10^{17} cm^{-3}) $In_{0.53}Ga_{0.47}As$ layers. The heavily doped (2.2×10^{19} cm^{-3}) top contact layers allows the formation of a low resistance non-alloyed ohmic contact.

2000Å	2.2 x 10^{19} cm^{-3}	$In_{0.53}Ga_{0.47}As$
3000Å	1.2 x 10^{17} cm^{-3}	$In_{0.53}Ga_{0.47}As$
50Å	UD	$In_{0.53}Ga_{0.47}As$
L	UD	BARRIER
50Å	UD	$In_{0.53}Ga_{0.47}As$
3000Å	1.2 x 10^{17} cm^{-3}	$In_{0.53}Ga_{0.47}As$
3000Å	2.2 x 10^{19} cm^{-3}	$In_{0.53}Ga_{0.47}As$
n+ InP Substrate		

Fig. 5. 6 Layer schematic diagram of the AlAs/$In_{0.53}Ga_{0.47}As$ structures studied. L denotes the thickness of the barrier layer and BARRIER represents its composition. For HBV I. L = 50Å and BARRIER = AlAs; HBV II: L = 100Å and BARRIER = AlAs; HBV III: L = 50Å/50Å/50Å and BARRIER = $In_{0.52}Al_{0.48}As$/AlAs/$In_{0.52}Al_{0.48}As$.

The J - V characteristics of the three structures are shown in Fig. 5.7. Although the J - V characteristics are quite symmetric, for clarity only one bias direction (positive voltage applied to the top contact) is shown. All three diodes exhibit excellent current blocking characteristics with breakdown voltages between 10 and 12 V with HBV I, the thinnest barrier device, having the lowest breakdown voltage. Since the J - V data is plotted on a linear scale, the difference in the characteristics at lower bias voltages is difficult to observe. Therefore, the data of Fig. 5.7 is re-plotted on a logarithmic scale in Fig. 5.8.

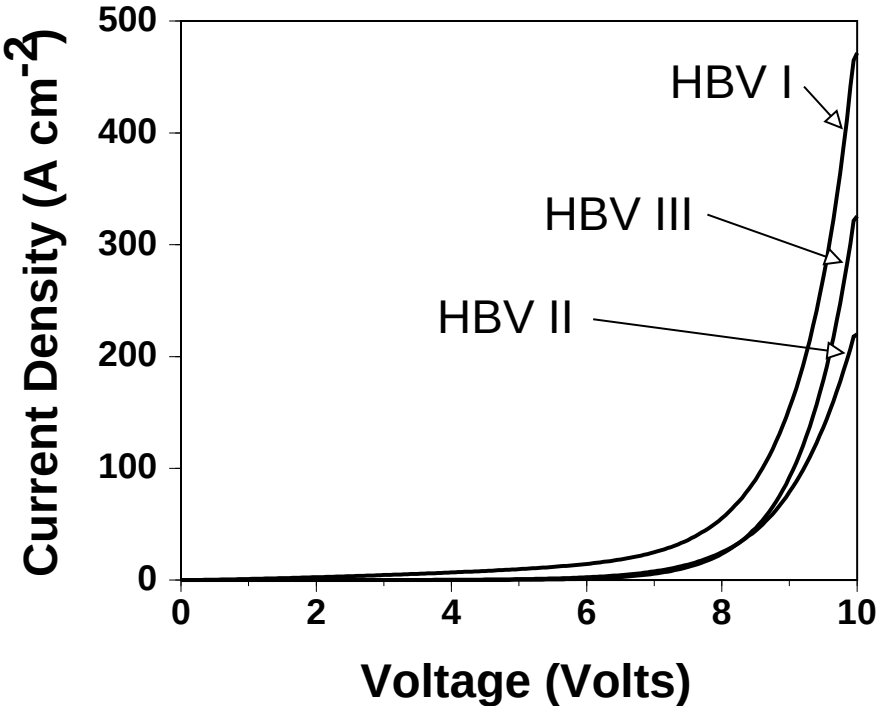

Fig. 5.7 J - V characteristics of AlAs/$In_{0.53}Ga_{0.47}As$ HBV diodes plotted on a linear scale.

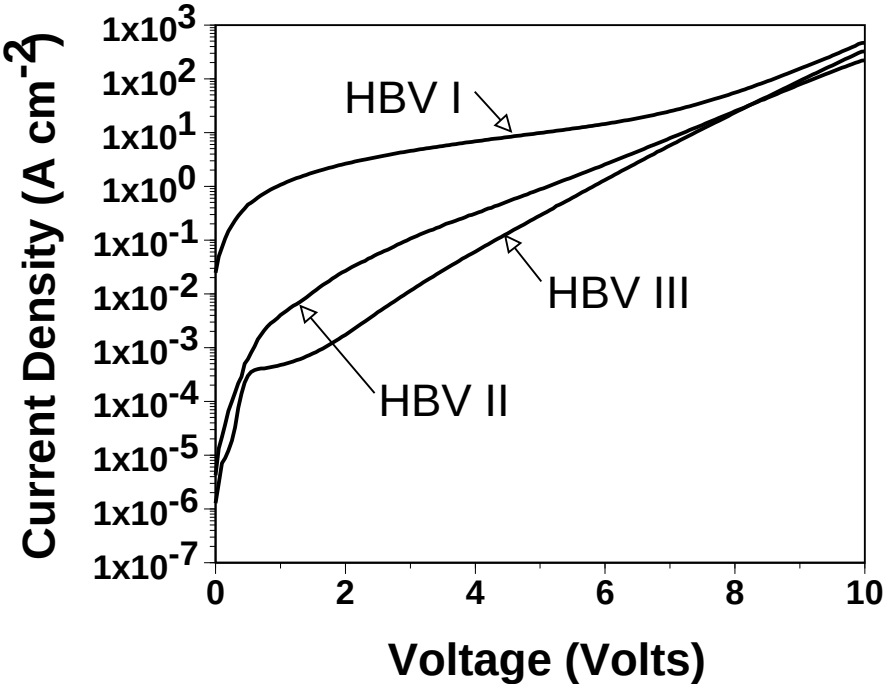

Fig. 5.8 J - V characteristics of AlAs/$In_{0.53}Ga_{0.47}As$ HBV diodes plotted on a logarithmic scale.

In Fig. 5.8 one can see more clearly the difference in the J - V characteristics of the three devices. For low voltages (less than 5 V) HBV II and III have current densities several orders of magnitude lower than HBV I. Only at voltages near breakdown do they exhibit similar current densities. For comparison, we plot in Fig. 5.9 J - V data from Nilsen *et al.* (from Chalmers University, Sweden) for HBV diodes fabricated in the AlGaAs/GaAs, $In_{0.52}Al_{0.48}As$ /$In_{0.53}Ga_{0.47}As$, and AlSb/InAs material systems [32]. The AlGaAs/GaAs HBV is identical to the one discussed in section 5.3. The $In_{0.52}Al_{0.48}As$ /$In_{0.53}Ga_{0.47}As$ HBV diode consists of a 250Å $In_{0.52}Al_{0.48}As$ barrier with 4000Å ($n = 6 \times 10^{16}$ cm^{-3}) $In_{0.53}Ga_{0.47}As$ depletion regions. The AlSb/InAs HBV device employs a 200Å AlSb barrier with 4000Å ($n = 1 \times 10^{17}$ cm^{-3}) InAs depletion regions.

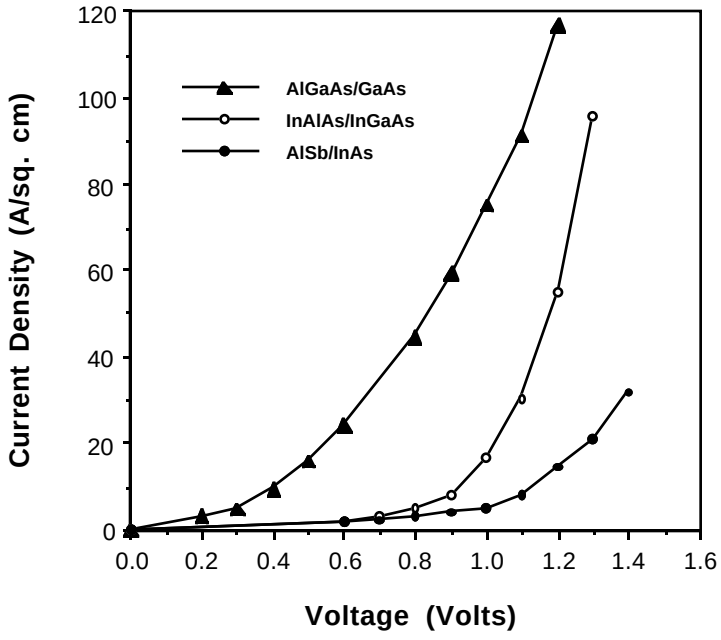

Fig. 5.9 J - V characteristics of AlGaAs/GaAs, $In_{0.52}Al_{0.48}As$ /$In_{0.53}Ga_{0.47}As$, and AlSb/InAs HBV diodes from Nilsen *et al.* [32}.

The breakdown voltages of the devices presented in Fig. 5.9 are very low, about 2 V. In contrast, the AlAs /$In_{0.53}Ga_{0.47}As$ HBV diodes presented in this work have breakdown voltages as high as 12 V. The AlSb/InAs HBV, which had the best current blocking characteristic of the devices shown in Fig. 5.9, exhibits a current density of 5 A cm^{-2} at 1 V. In comparison, HBV III has a current density of only 4 x 10^{-4} A cm^{-2} at 1 V, reaching a current density of 5 A cm^{-2} at approximately 7 V. Therefore, the AlAs /$In_{0.53}Ga_{0.47}As$ HBV diodes presented in this work have the highest breakdown voltages reported to date. It should also be pointed out that the AlAs /$In_{0.53}Ga_{0.47}As$ HBV diodes have shorter depletion regions (3000Å compared to 4000Å) and higher dopant concentrations in the depletion region compared to the diodes reported by Nilsen *et al.*.

We have discussed until now the current blocking characteristics of HBV diodes since as it is their major limitation. However, the device characteristic of interest is, of course, the C - V characteristic. Shown in Fig. 5.10 are the C - V characteristics of the AlAs /$In_{0.53}Ga_{0.47}As$ HBV diodes. As expected, the curves are symmetric about the voltage axis and the zero-bias capacitance increases as the barrier thickness decreases. The C_{max}/C_{min} ratio varies from 6 for QBV I to 4 for QBV III.

Shown in Fig. 5.11 are the G/C ratio versus voltage characteristics for the AlAs/$In_{0.53}Ga_{0.47}As$ HBV diodes. Recall from Eq. 5.5 that the characteristic frequency G/C should be as low as possible for a good varactor. As expected, HBV I, the thinnest barrier device, exhibits the highest characteristic frequencies with HBV III exhibiting the lowest. The noise in the HBV III data is due to noise in the conductance data. For larger voltages (greater than 3 V) the conductance begins to increase for all three devices and the characteristic frequency increases.

The cutoff frequency, f_c, of HBV III is calculated, from Eq. 5.4, to be approximately 1.2 THz. This calculation assumes a conservative specific ohmic

contact resistance of 10^{-6} ohm-cm^2 and that the depletion regions on both sides are undepleted.

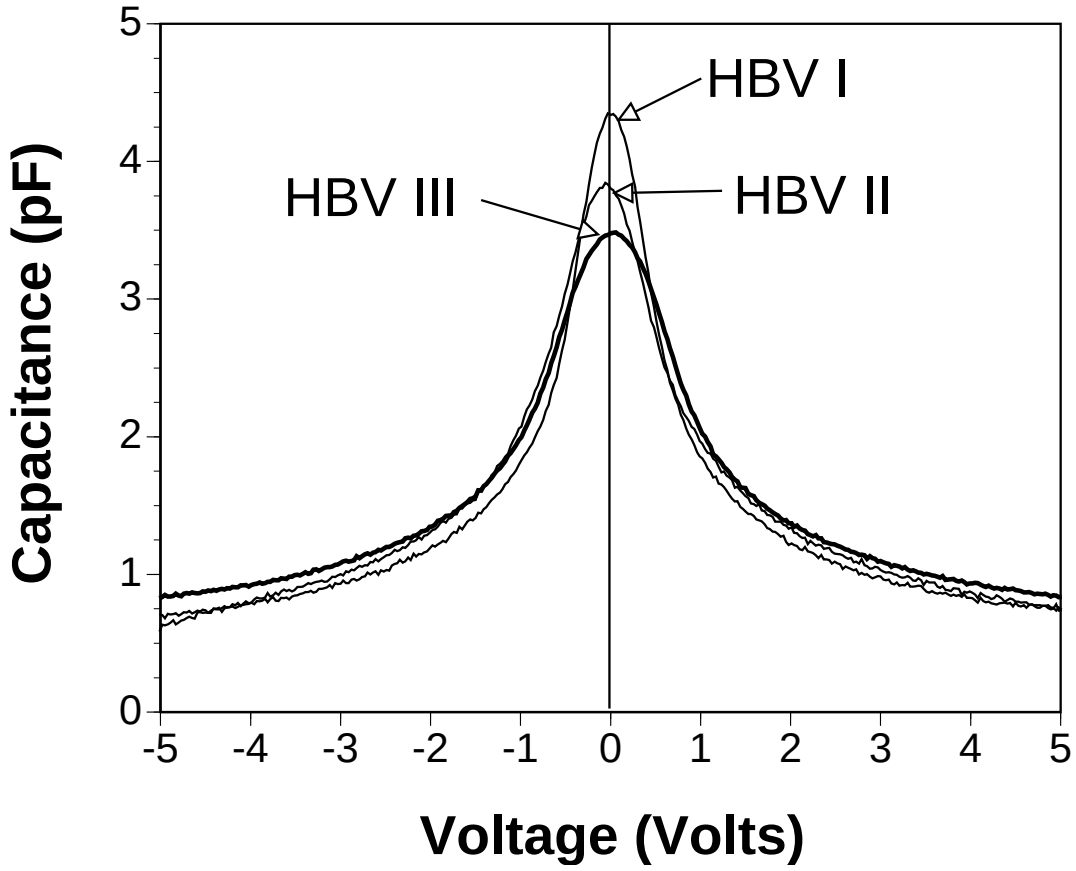

Fig. 5. 10 C - V characteristics of AlAs /$In_{0.53}Ga_{0.47}As$ HBV diodes.

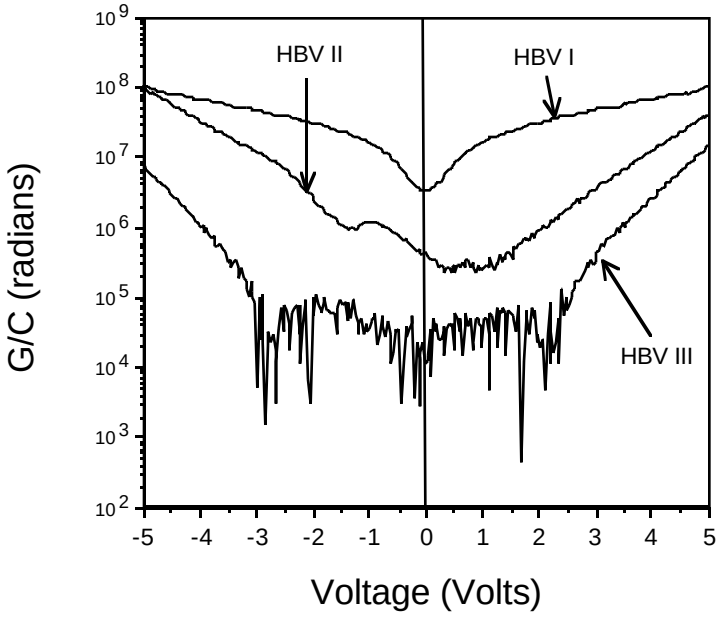

Fig. 5.11 G/C versus Voltage characteristics of AlAs/$In_{0.53}Ga_{0.47}As$ HBV diodes.

5.6 Summary

We have briefly described the technique of frequency multiplication with a varactor diode. This is an alternate approach for generating useful amounts of submillimeter-wavelength radiation. The dominant semiconductor device presently used for such applications is the Schottky barrier diode. However, since all higher order harmonics are generated with a Schottky diode varactor, difficult idler circuit design is required. The HBV diode, which possesses even symmetry in the C - V characteristics, is a potential replacement for submillimeter-wavelength Schottky diode varactors. The reduced number of harmonics generated with the HBV diode significantly relax the multiplier circuit design requirements. The major problem with this type of device has been its low breakdown voltage and excessive conduction current which leads to low multiplier power conversion efficiency. We have presented results on AlGaAs/GaAs and AlAs/$In_{0.53}Ga_{0.47}As$ HBV diodes which exhibit record breakdown voltages as high as 12 V and capacitance modulation ratios as high as 6. The AlAs/$In_{0.53}Ga_{0.47}As$ HBV diodes, in particular, are extremely attractive candidates for submillimeter wavelength frequency multipliers.

References

[1] Chester H. Page, " Harmonic generation with ideal rectifiers," Proc. of the IRE, vol. 46, pp.1738-1740, 1958.

[2] J. M. Manley and H. E. Rowe, " Some general properties of nonlinear elements - Pt I, general energy relations," Proc. IRE, vol. 44, pp.904-913, 1956.

[3] T. J. Tolmunnen and M. A. Frerking, " Theoretical performance of novel multipliers at millimeter and submillimeter wavelengths," Int. Journal of Infrared and Millimeter Waves, vol. 12, No. 10, pp.1111-1133, 1991.

[4] Stephen A. Maas, " Nonlinear Microwave Circuits," Artech House, Norwood, Massachusetts, 1988.

[5] A. R. Kerr, " A technique for determining the local oscillator waveforms in a microwave mixer," IEEE Trans. on Microwave Theory and Tech., vol. 28, No. 10, pp.828-831, 1975.

[6] H. A. Watson, ed., " Microwave Semiconductor Devices and Their Circuit Applications," McGraw Hill, New York, 1969.

[7] S. M. Sze, " Physics of Semiconductor Devices," John Wiley, New York, 1981.

[8] U. Lieneweg, T. J. Tolmunnen, M. A. Frerking, and J. Maserjian, " Modeling of Planar Varactor Frequency Multiplier Devices with Blocking Barriers," IEEE Trans. on Microwave Theory and Tech., vol. 40, No. 5, pp.839-845, 1992.

[9] W. C. B. Peatman, T. W. Crowe, and M. Shur, " A Novel Schottky/2-Deg Diode for Millimeter- and Submillimeter-Wave Multiplier Applications," vol. 13, No. 1, pp.11-13, 1992.

[10] R. J. Hwu and L. P. Sadwick, " Limitations of the Back-to-Back Barrier-Intrinisc-n+ (BIN) Diode Frequency Tripler," IEEE Trans. on Electron Devices, vol. 39, No. 8, pp.1805-1810.

[11] W. C. B. Peatman, P. A. D. Wood, D. Porterfield. T. W. Crowe, and M. J. Rooks, " Quarter-Micrometer GaAs Schottky barrier diode with high video responsivity at 188 μm," Appl. Phys. Lett., vol. 61, No. 3, pp.294-296, 1992.

[12] N. Erickson, " High Efficiency Submillimeter Frequency Multipliers," Proc. of 1990 MTT-S Digest, pp. 1301-1304, 1990.

[13] A. Rydberg, B. N. Lyons, and S. U. Lidholm, " On the development of a high efficiency 750 GHz frequency tripler for THz heterodyne systems," IEEE Trans. on Microwave Theory and Tech., vol. 40, No. 5, pp.827-830, 1992.

[14] E. Kollberg and A. Rydberg, " Quantum Barrier Varactor Diodes for high-efficiency millimetre-wave multipliers," Electronics Lett., vol. 25, No. 25, pp.1696-1698, 1989.

[15] T. C. L. G. Sollner, E. R. Brown, and H. Q. Le, " Microwave and Millimeter-Wave Resonant Tunneling Devices," The Lincoln Laboratory Journal, vol. 1, No. 1, pp.89-106, 1988.

[16] P. D. Batelaan and M. A. Frerking, " Quantum Well Multipliers," Proc. of 12th International Conf. on Infrared and Millimeter Waves, pp.14-15, 1987.

[17] P. D. Batelaan, T. J. Tolmunnen, and M. A. Frerking, " Quantum-Well Diode Frequency Multipliers: Varistor Case," IEEE Micro. and Guided Wave Lett., vol. 2, No. 7, pp.289-291, 1992.

[18] B. J. Rizzi, T. W. Crowe, and N. R. Erickson, " A High-Power Millimeter-Wave Frequency Doubler Using a Planar Diode Array," IEEE Micro. and Guided Wave Lett., vol. 3, No. 6, pp.188-190, 1993.

[19] A. Rydberg, H. Gronqvist, and E. Kollberg, " Millimeter- and Submillimeter-Wave Multipliers Using Quantum-Barrier-Varactor (QBV) Diodes," IEEE Electron Device. Lett., vol. 11, No. 9, pp.373-375, 1990.

[20] D. Choudhury, M. A. Frerking, and P. D. Batelaan, " A 200 GHz Tripler Using a Single Barrier Varactor," IEEE Trans. on Microwave Theory and Tech., vol. 41, No. 4, pp.595-599, 1993.

[21] H. X. L. Liu, L. B. Sjogren, C. W. Dohmier, N. C. Luhmann, D. L. Sivco, and A. Y. Cho," Monolithic quasi-optical frequency tripler array with 5-W output power at 99 GHz," IEEE Electron Device Lett., vol. 14, No. 7, pp.329-331, 1993.

[22] P. W. Staecker, M. E. Hines, F. Occhiuti, and J. F. Cushman, " Multi-watt power generation at millimeter-wave frequencies using epitaxially-stacked varactor diodes," 1987 IEEE MTT-S Digest, pp.917-920, 1987.

[23] Antii V. Raisanen, " Frequency multipliers for millimeter and submillimeter wavelengths," Proc. of the IEEE, vol. 80, No. 11, pp.1842-1852, 1992.

[24] K. Krishanmurthi and R. G. Harrison, " Comments on " Millimeter-Submillimeter-Wave Multipliers Using Quantum-Barrier-Varactor (QBV) Diodes," IEEE Electron Device Lett., vol. 13, No. 2, p.132, 1992.

[25] M. Rossmanith, J. Leo, and K. von Klitzing," Model of G-X transition in thermally activated tunnel current across $Al_xGa_{1-x}As$ single barriers," J. Appl.

Phys., vol. 69, No. 6, pp.3641-3645, 1991.

[26] T. W. Crowe, W. C. B. Peatman, and E. Winkler, " GaAs Schottky Barrier Varactor Diodes for submillimeter wavelength power generation," Microwave and Optical Tech. Lett., vol. 4, No. 1, pp.49-53, 1991.

[27] S. Adachi, " GaAs, AlAs, and $Al_xGa_{1-x}As$: Material parameters for use in research and device applications," J. Appl. Phys., vol. 58, No. 3, pp.R1-R@(, 1985.

[28] F. W. Smith, A. R. Calawa, C. Chen, M. J. Manfra, and L. J. Mahoney, " New MBE Buffer Used to Eliminate Backgating in GaAs MESFETs," IEEE Electron Device Lett., vol. 9, No. 1, pp.77-80, 1988.

[29] G. L. Witt, R. Calawa, U. Mishra, and E. Weber, " Low Temperature (LT) GaAs and Related Materials," MRS Proc., vol. 241, 1992.

[30] T. J. Rogers, C. Lei, B. G. Streetman, and D. G. Deppe, " Low growth temperature AlGaAs current blocking layers for use in surface normal optoelectronic devices," J. Vac. Sci. Tech. B, vol. 11, No. 3, pp.926-928, 1993.

[31] T. Y. Chu, A. Dodabalapur, A.Srinivasan, D. P. Neikirk, and B. G. Streetman, " Properties and Applications of $Al_xGa_{1-x}As$ ($0<x<1$) Grown at Low Temperatures," J. Crystal Growth, vol. 111, pp.26-29, 1991.

[32] S. M. Nilsen, H. Gronqvist, H. Hjelmgren, A. Rydberg, and E. L. Kollberg, " Single Barrier Varactors for Submillimeter Wave Power Generation," IEEE Trans. on Micro. Wave Theory and Tech., vol. 41, No. 4, pp.572-580, 1993.